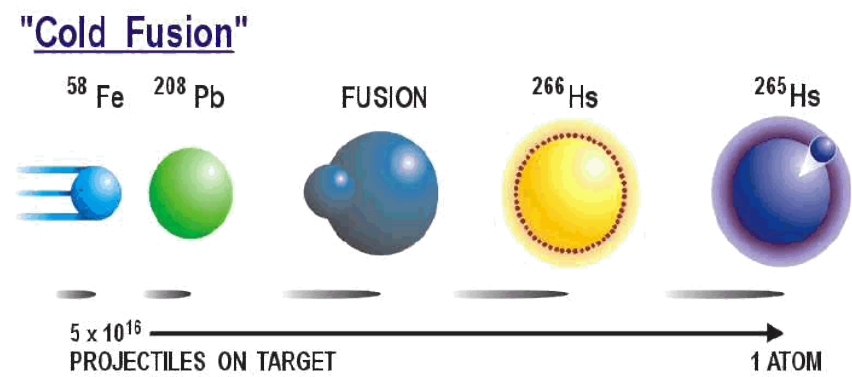
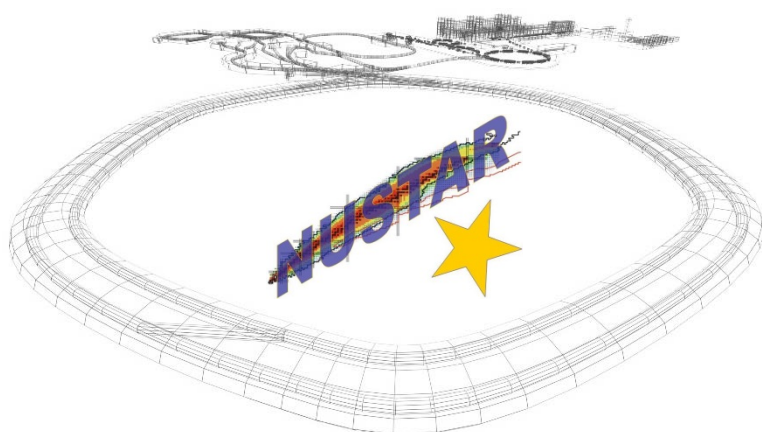


Spectrometer – particle identification

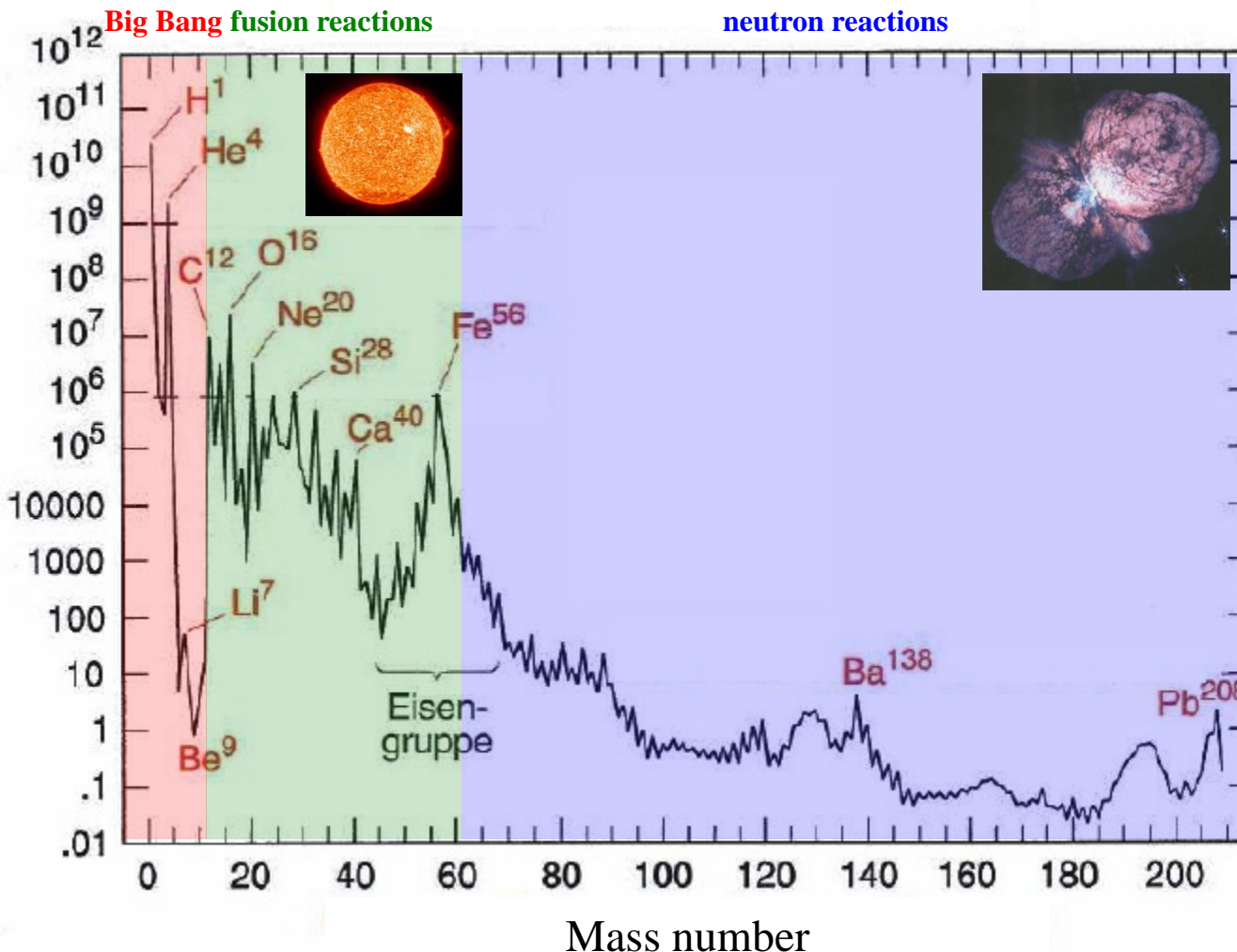
Lecture: Hans-Jürgen Wollersheim

e-mail: h.j.wollersheim@gsi.de



Solar abundances of elements

Solar abundance ($\text{Si}^{28} = 10^6$)



open questions:

- Why is Fe more common than Au ?
- Why do the heavy elements exist and how are they produced?
- Can we explain the solar abundances of the elements?

The chart of nuclides

Nucleosynthesis in the r-process

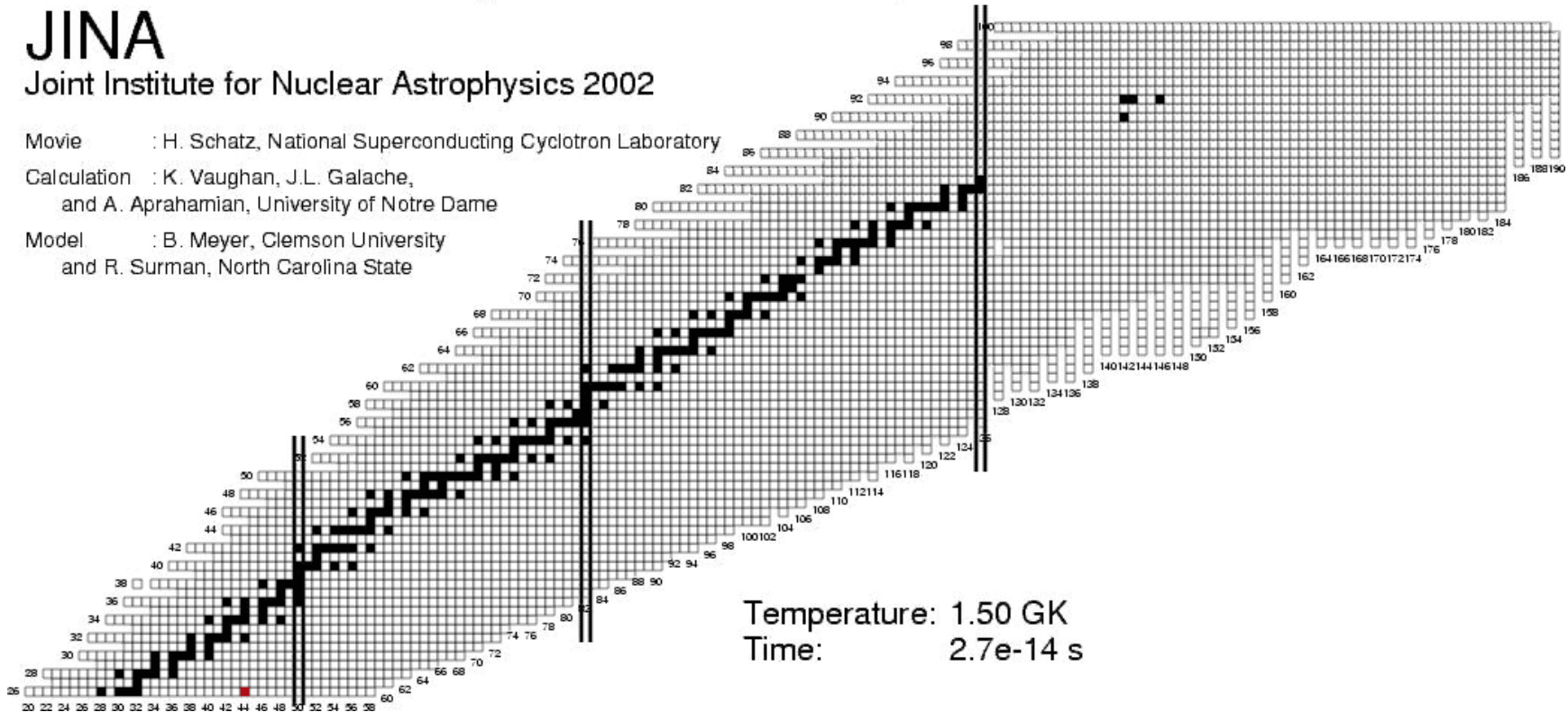
JINA

Joint Institute for Nuclear Astrophysics 2002

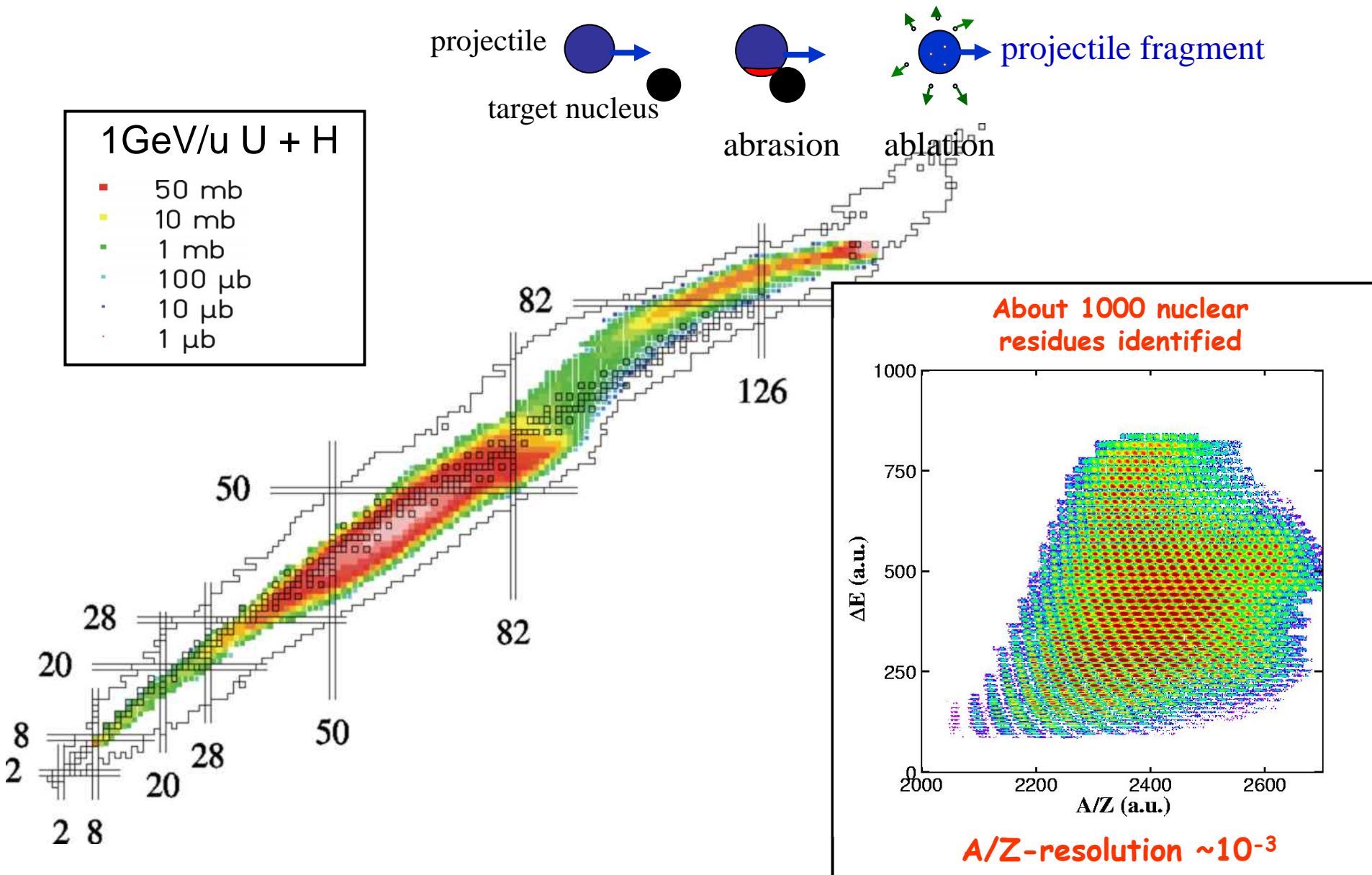
Movie : H. Schatz, National Superconducting Cyclotron Laboratory

Calculation : K. Vaughan, J.L. Galache,
and A. Aprahamian, University of Notre Dame

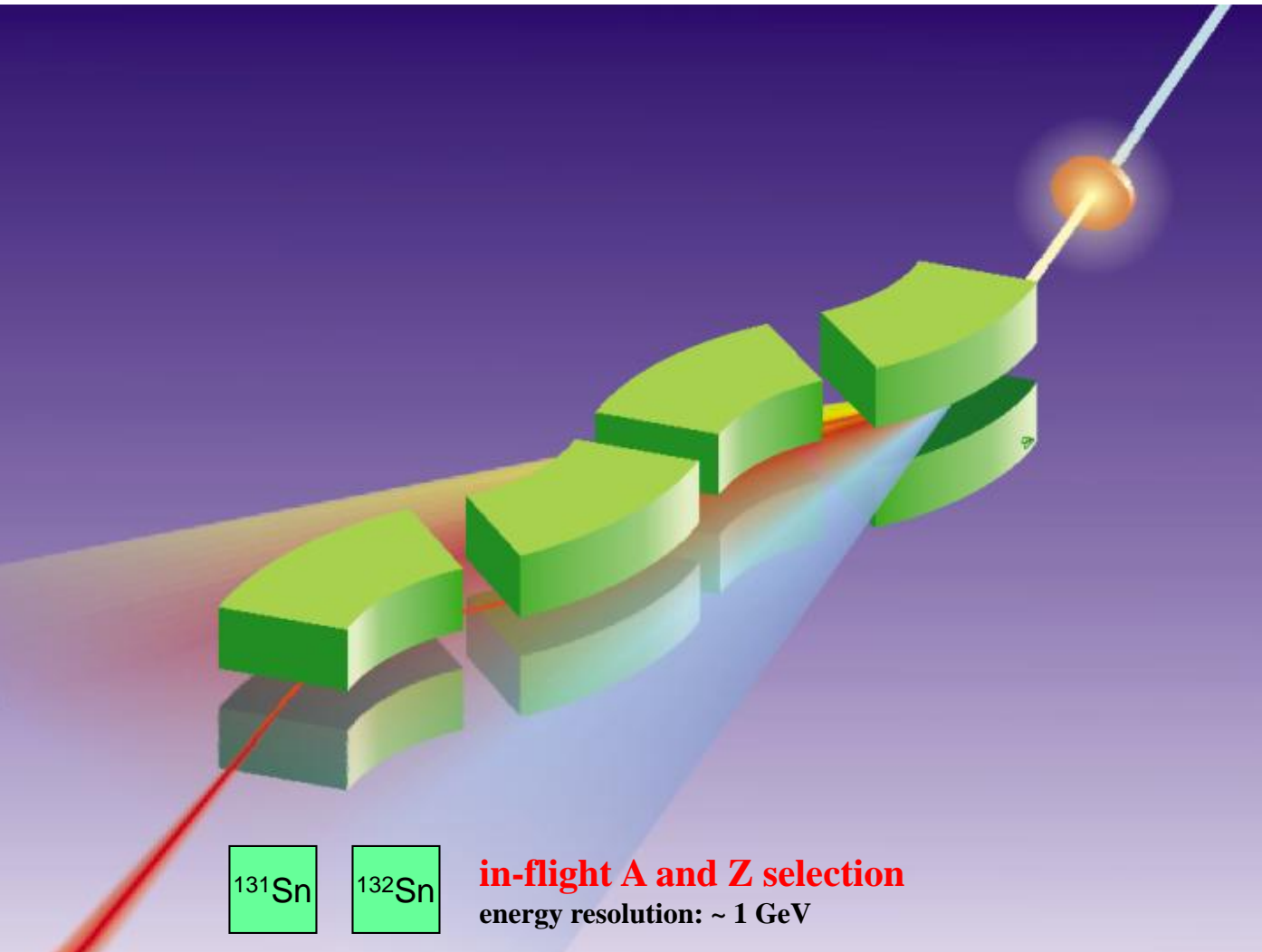
Model : B. Meyer, Clemson University
and R. Surman, North Carolina State



Radioactive Ion Beams at GSI

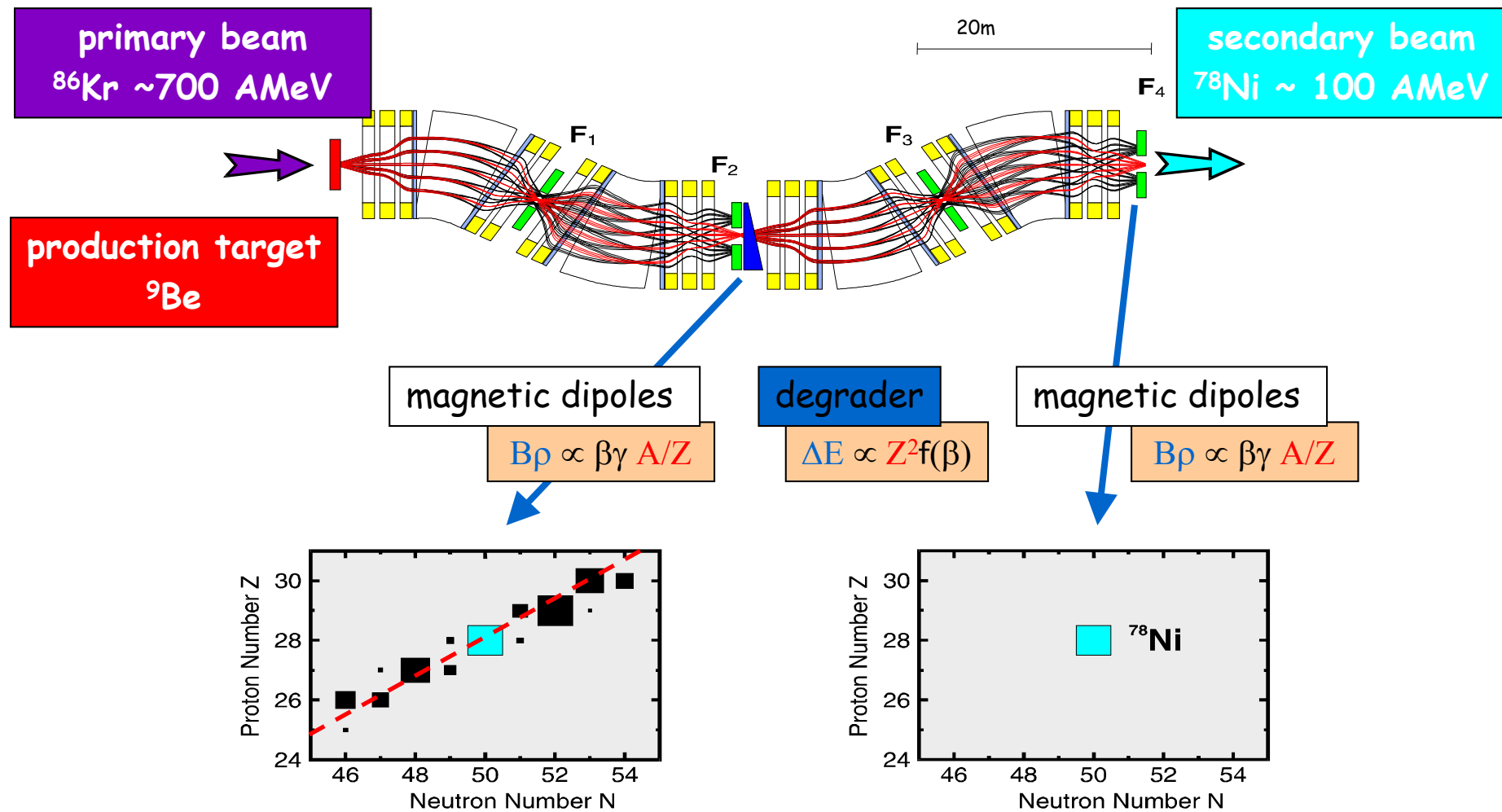


FFragment Separator at GSI

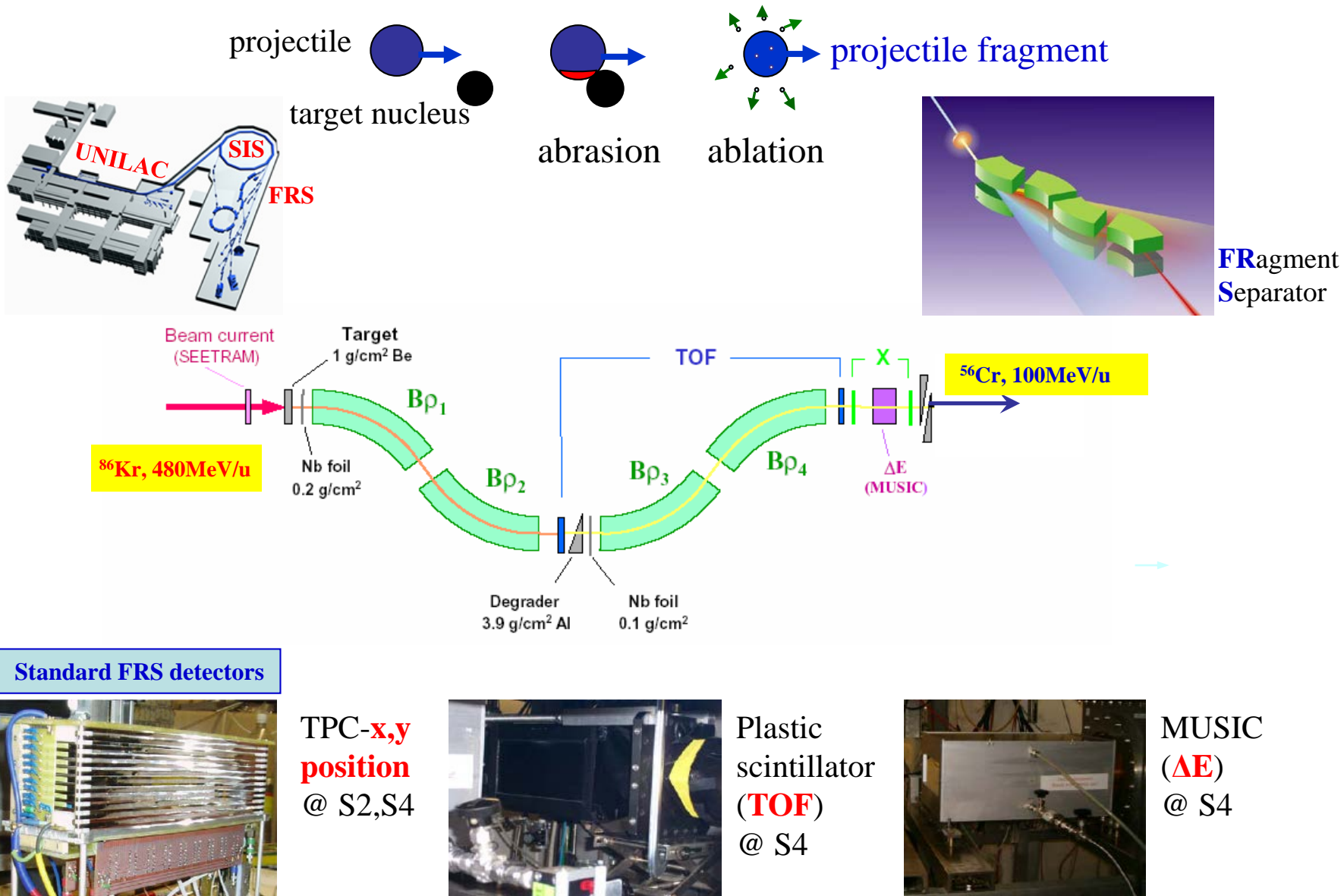


in-flight A and Z selection
energy resolution: ~ 1 GeV

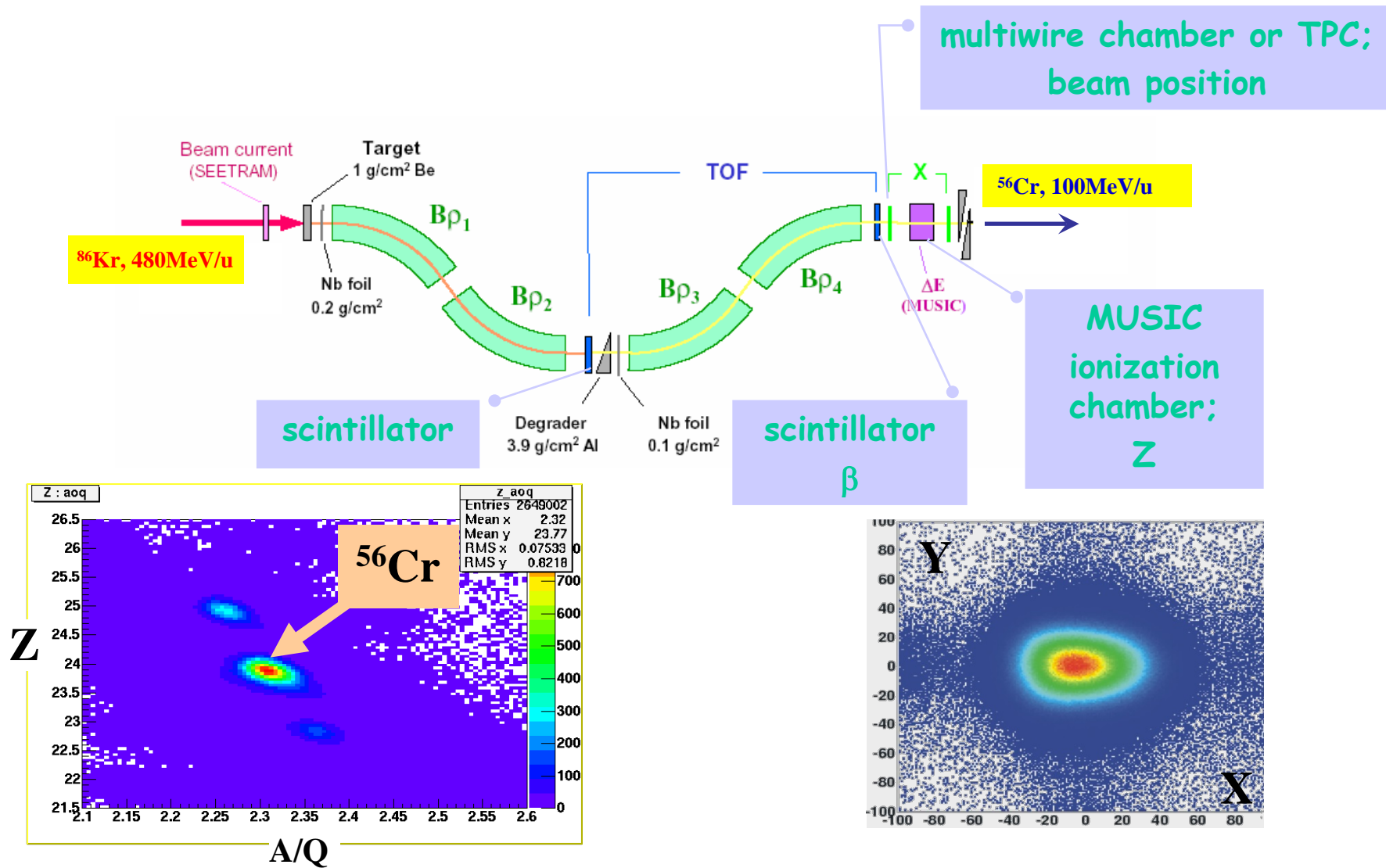
Rare Isotope Selection at FRS: $B\rho - \Delta E - B\rho$ selection



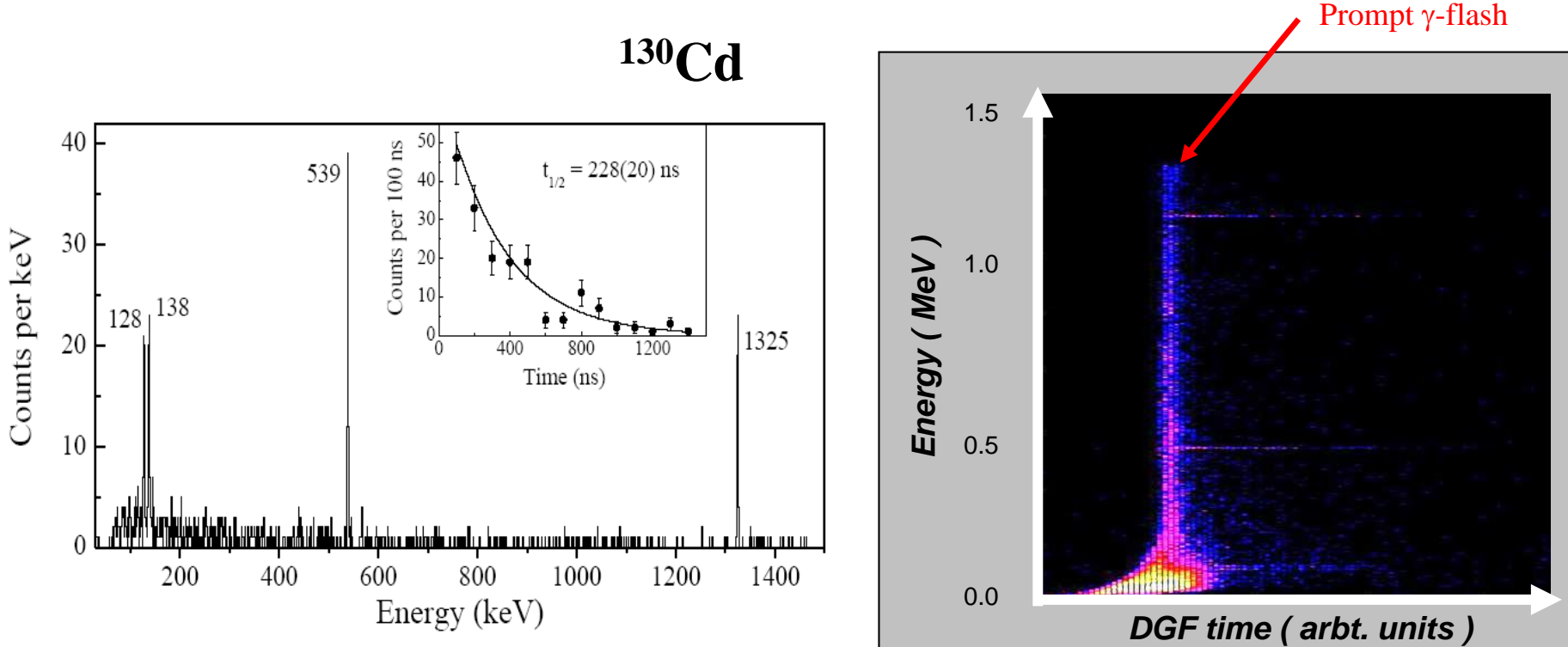
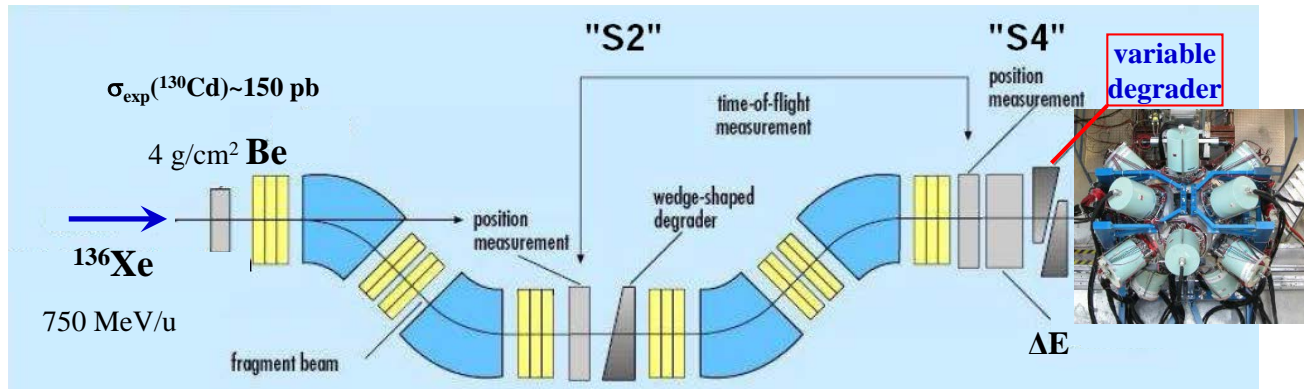
Production, Separation, Identification

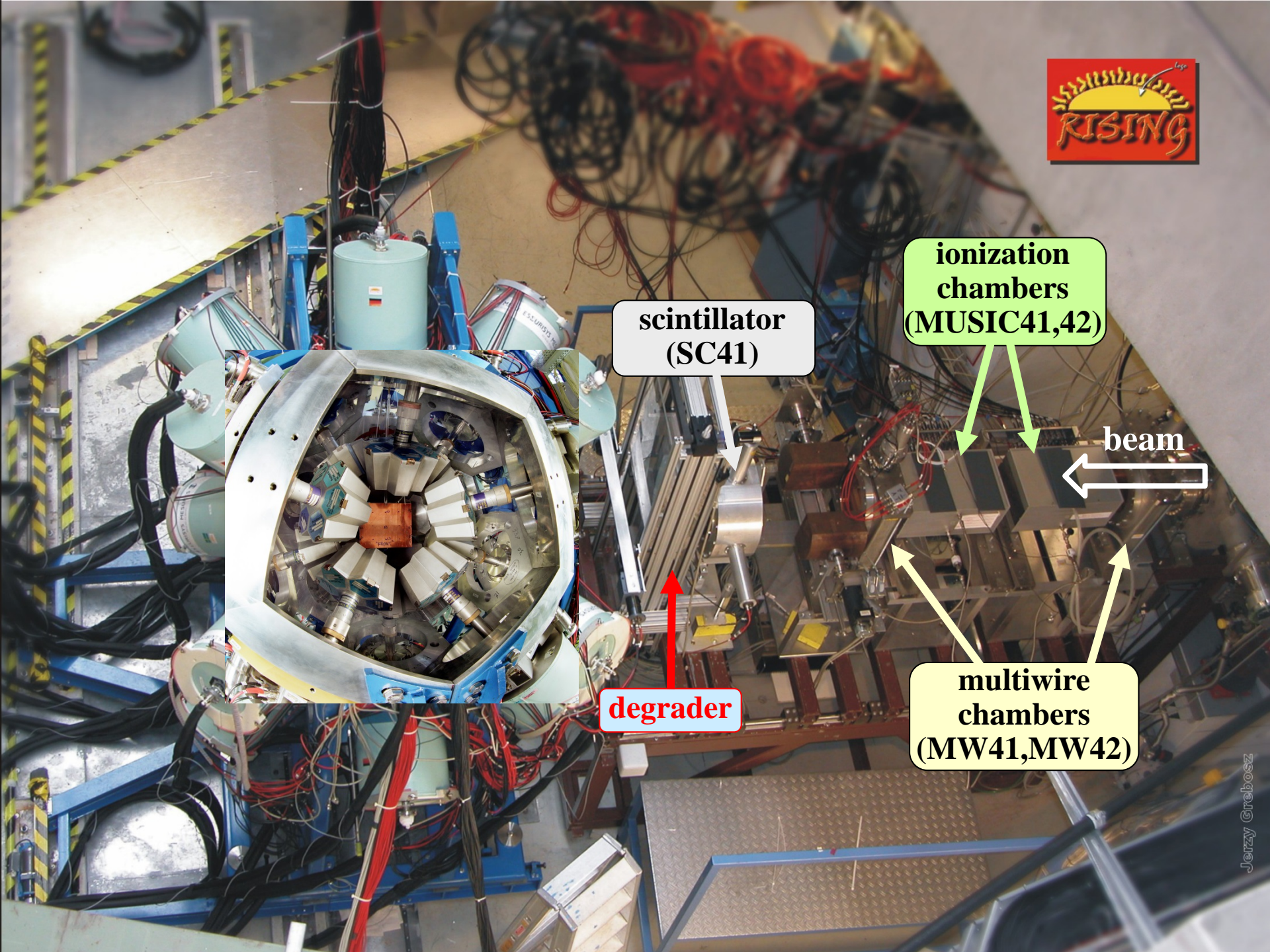


Production, Separation, Identification

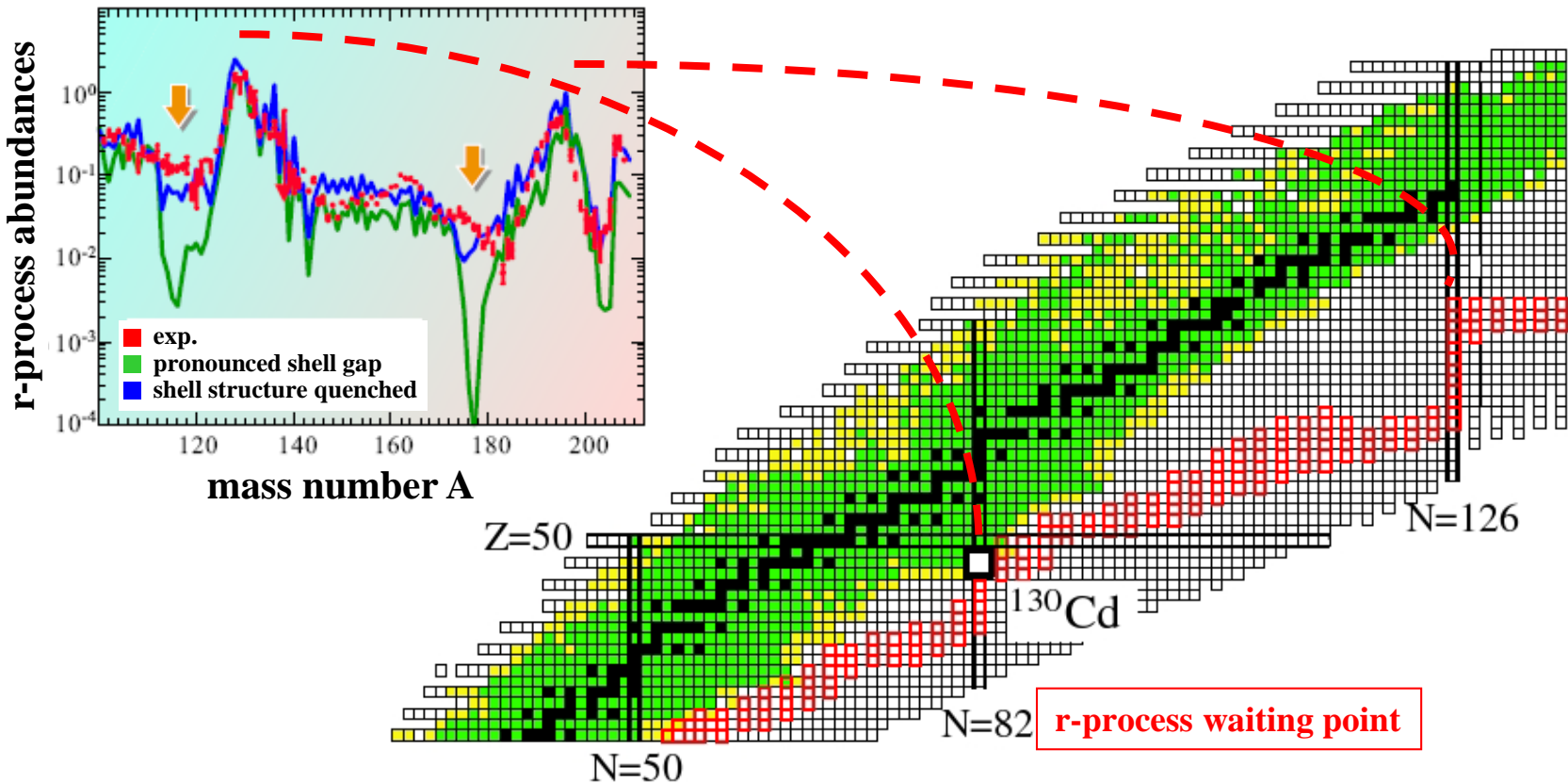


Experimental set-up for γ -ray spectroscopy



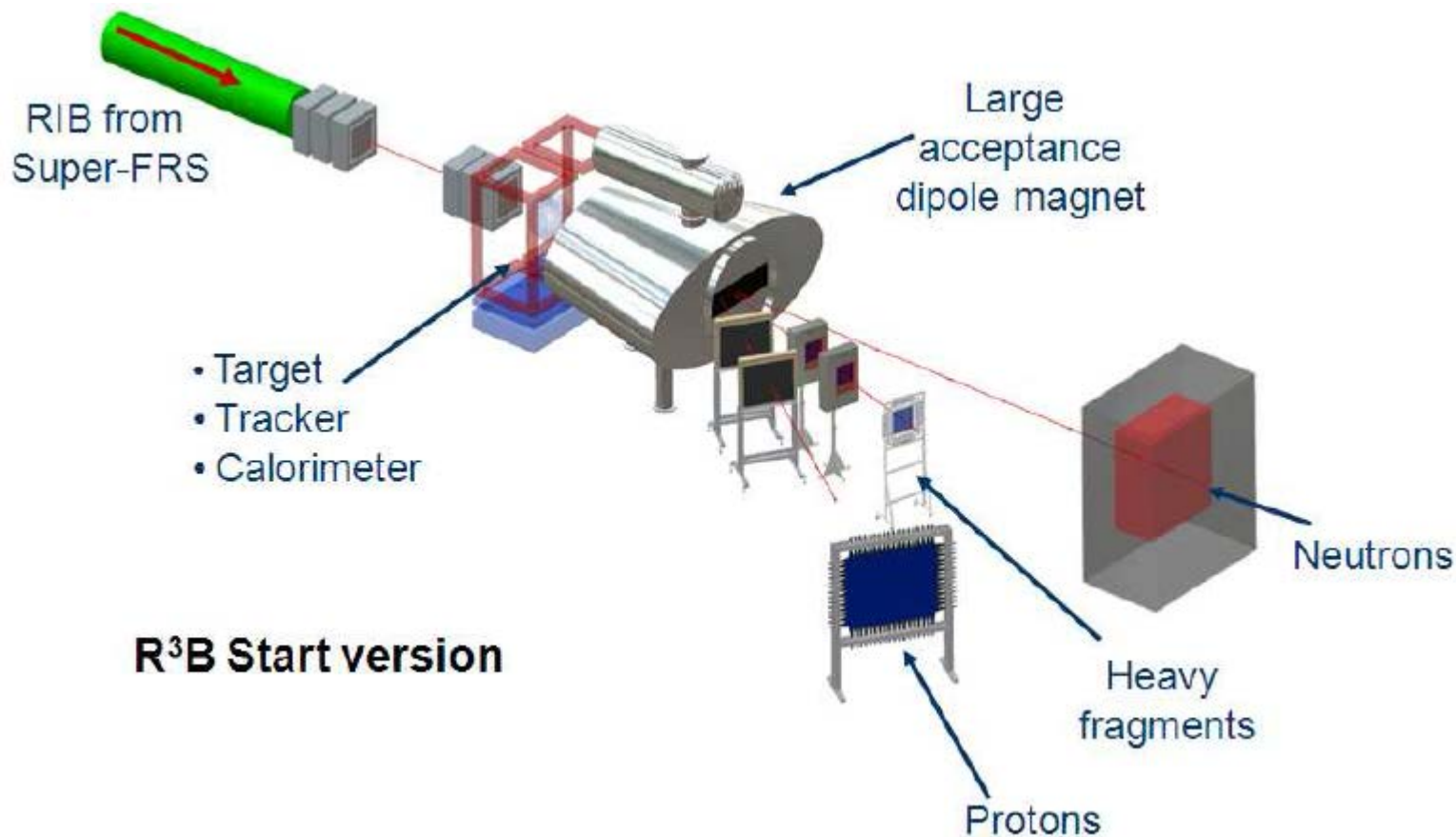


The astrophysical r-process 'path'



Assumption of a $N=82$ shell quenching leads to a considerable improvement in the global abundance fit in r-process calculations !

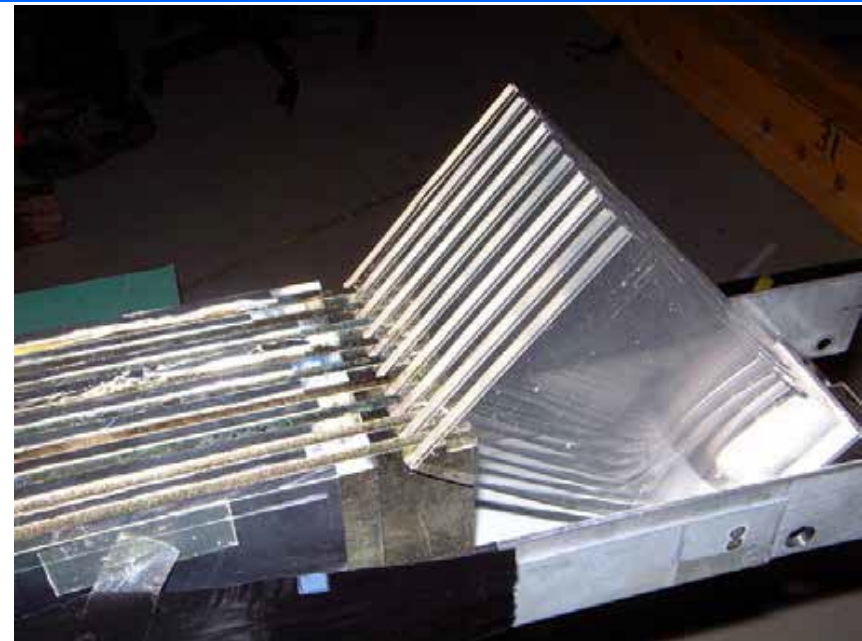
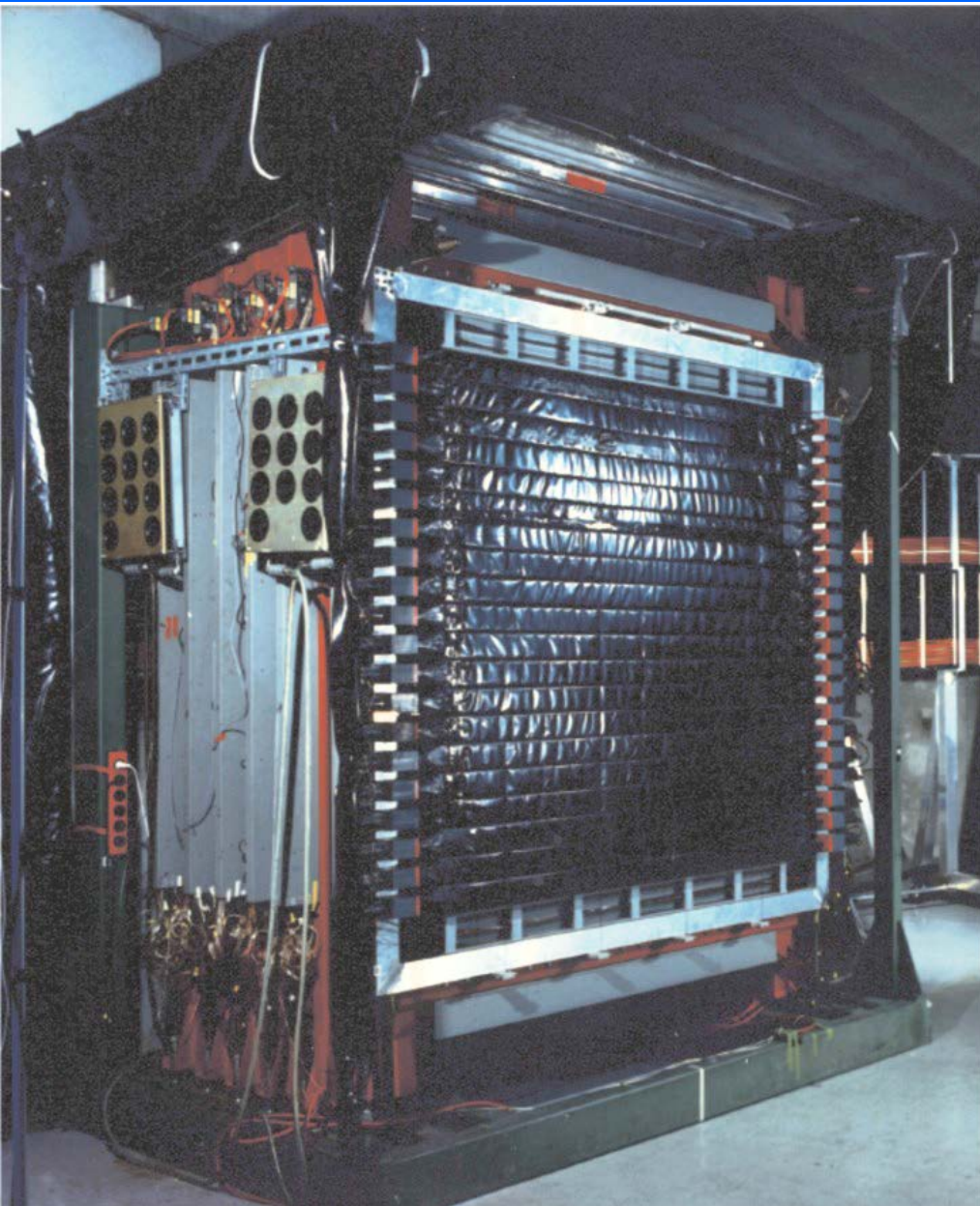
Reaction with Relativistic Radioactive Beams – R³B



Excitation energy E* from kinematically complete measurement of all outgoing particles

$$E^* = \left(\sqrt{\sum_i m_i^2 + \sum_{i \neq j} m_i m_j \gamma_i \gamma_j (1 - \beta_i \beta_j \cos \vartheta_{ij})} - m_{proj} \right) c^2 + E_{\gamma,sum}$$

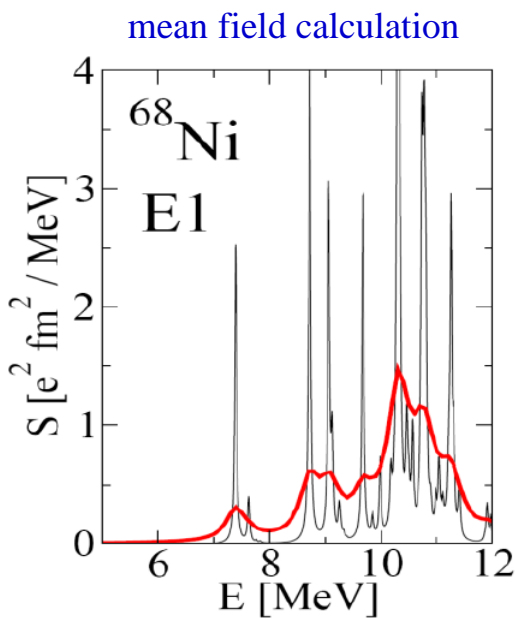
Large Area Neutron Detector



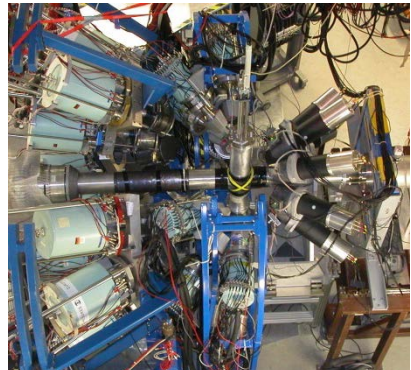
Large Area Neutron Detector (2m x 2m x 1m)

- neutron energy $T_n \leq 1 \text{ GeV}$
- $\Delta T_n/T_n = 5.3\%$
- efficiency ~ 1
- passive Fe-converter

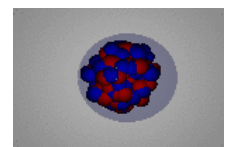
Dipole strength distribution of ^{68}Ni



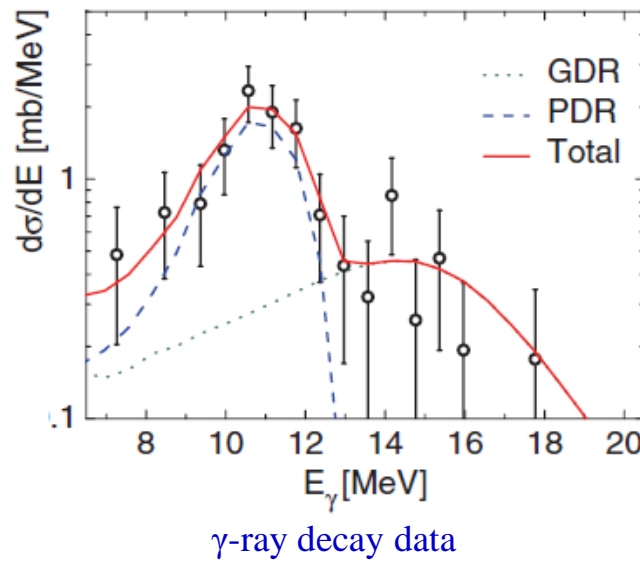
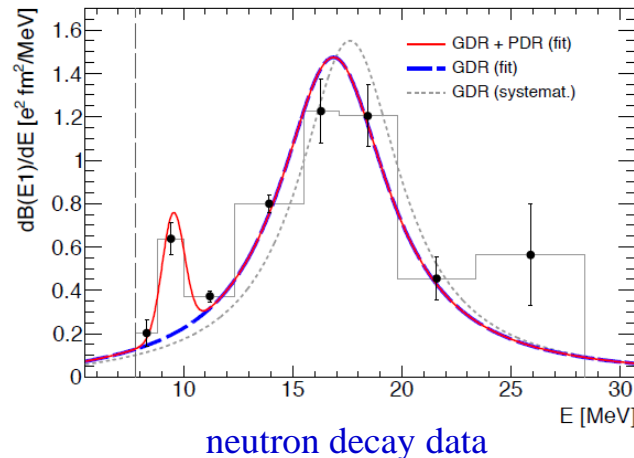
E.Litvinova et al.; PRC 79, (2009) 054312



O. Wieland et al.; Phys. Rev. Lett 102, 092502 (2009)



Pygmy resonance

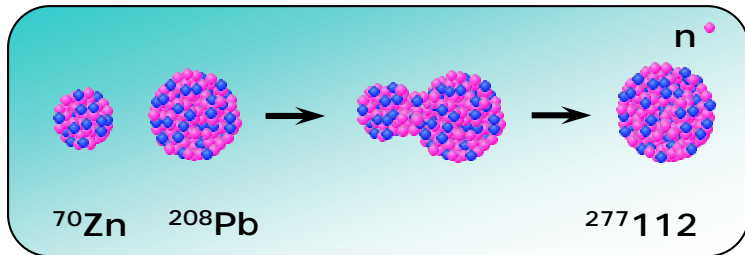


D. Rossi et al.; Phys. Rev. Lett 111, 242503 (2013)

direct γ -decay
branching ratio:

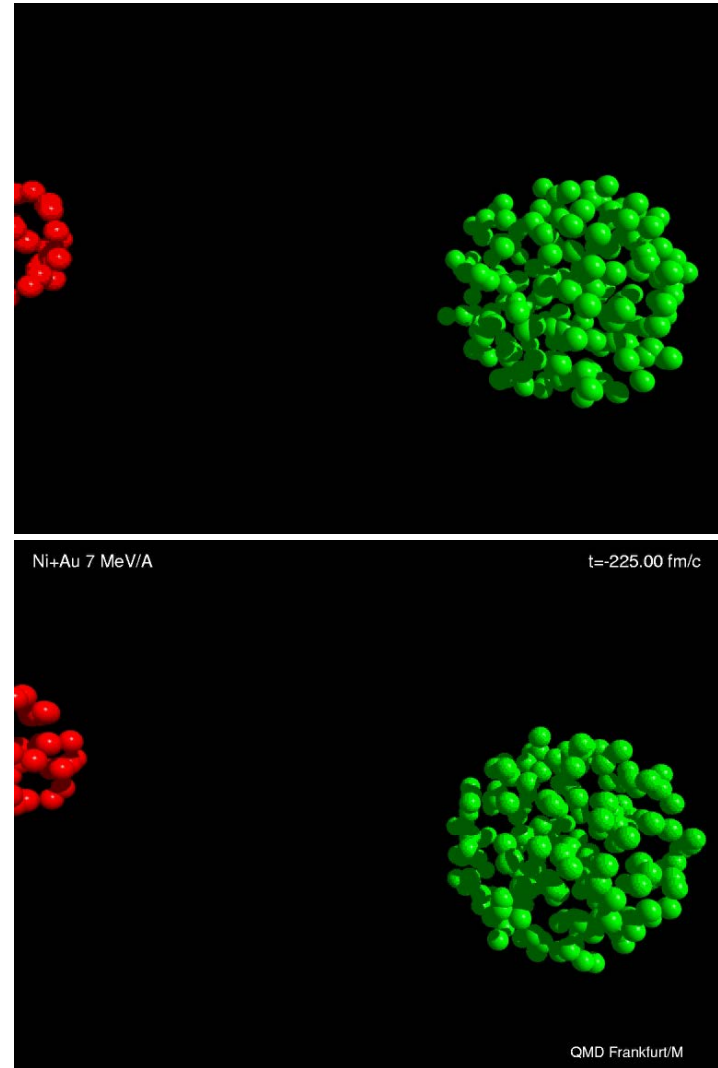
$$\Gamma_0/\Gamma = 7(2)\%$$

Synthesis of heavy elements

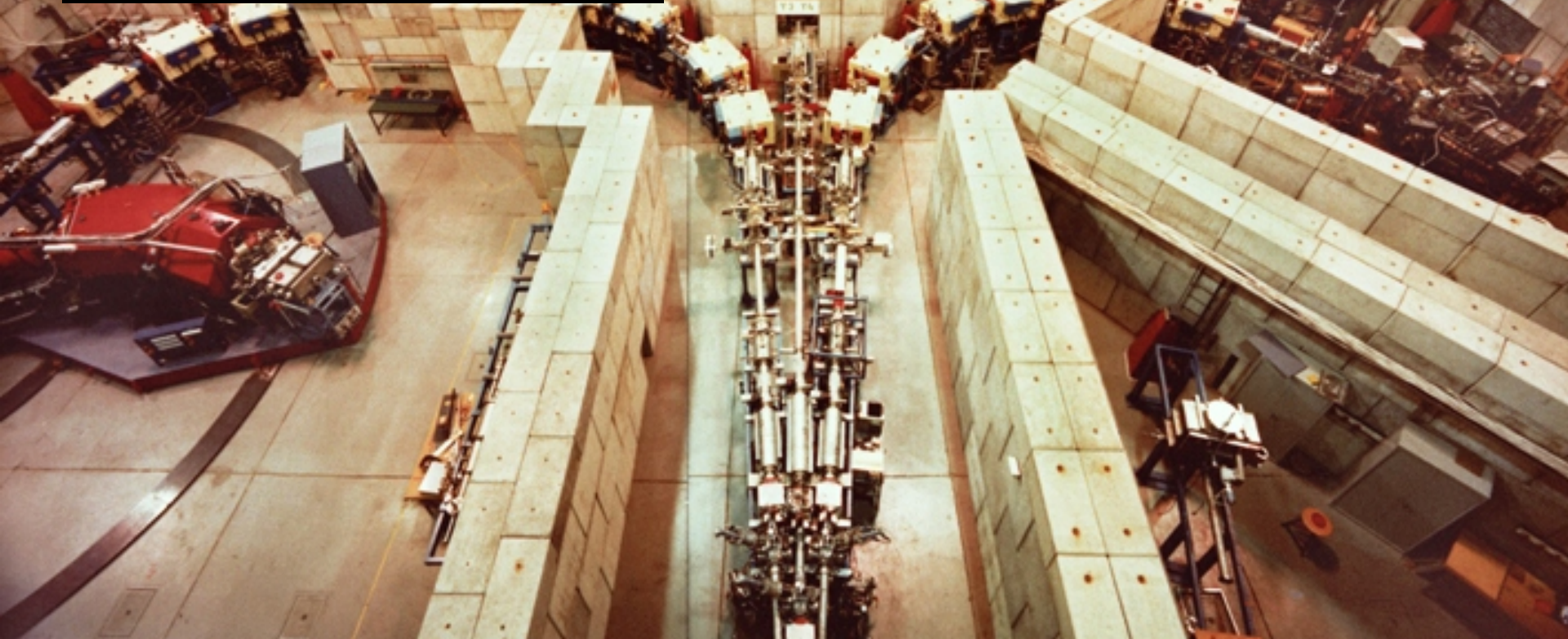


Fusion

$$-\frac{1}{10^{12}}$$



Separator for Heavy Ion Products (SHIP)



Separator for Heavy Ion Products (SHIP)

- Fusion products are slower than scattered or transfer particles

$$v_{CN} = [m_p/(m_p + m_t)] \cdot v_p$$

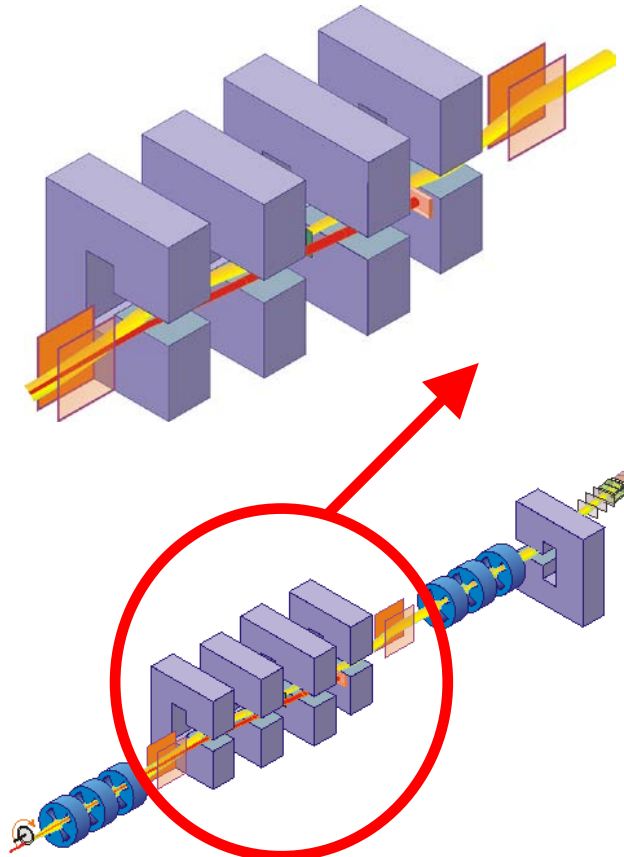
$$e \cdot q \cdot v_p \approx 10.3\% \rightarrow v_{CN} \approx 2.2\%$$

- E- and B-field are perpendicular to each other

$$B \cdot \rho = \frac{m \cdot v}{e \cdot q}$$

$$E \cdot \rho = \frac{m \cdot v^2}{e \cdot q}$$

$$F_{mag} = F_{el} \Rightarrow F_{tot} = 0$$



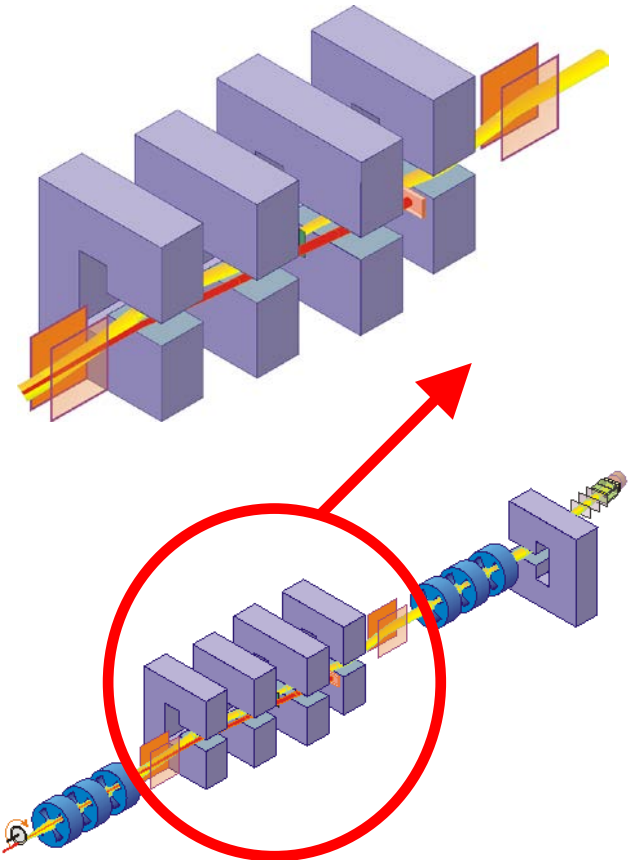
electric deflectors: ± 330 kV dipole magnets: 0.7 T max

Separator for Heavy Ion Products (SHIP)

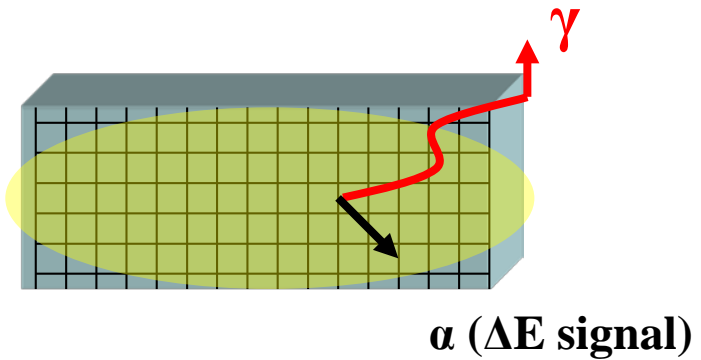
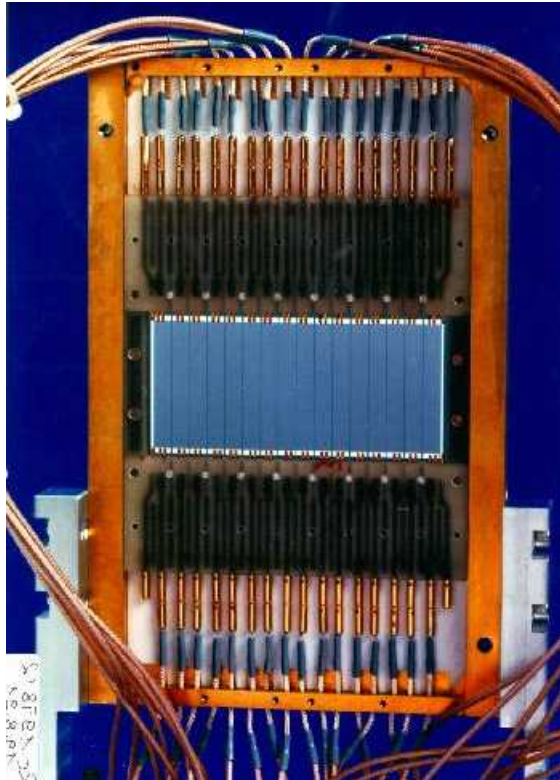
- The choice of E and B determines the transmitted velocity

$$v = \frac{E}{B}$$

- The rejected beam will be stopped on a cooled Cu plate



SHIP – stop detector



SHE will be measured in a pixel

- position sensitive Silicon detector determines the position and energy of SHE and α , β , ...

area: $27 \times 87 \text{ mm}^2$, thickness: 0.3mm, 16 strips

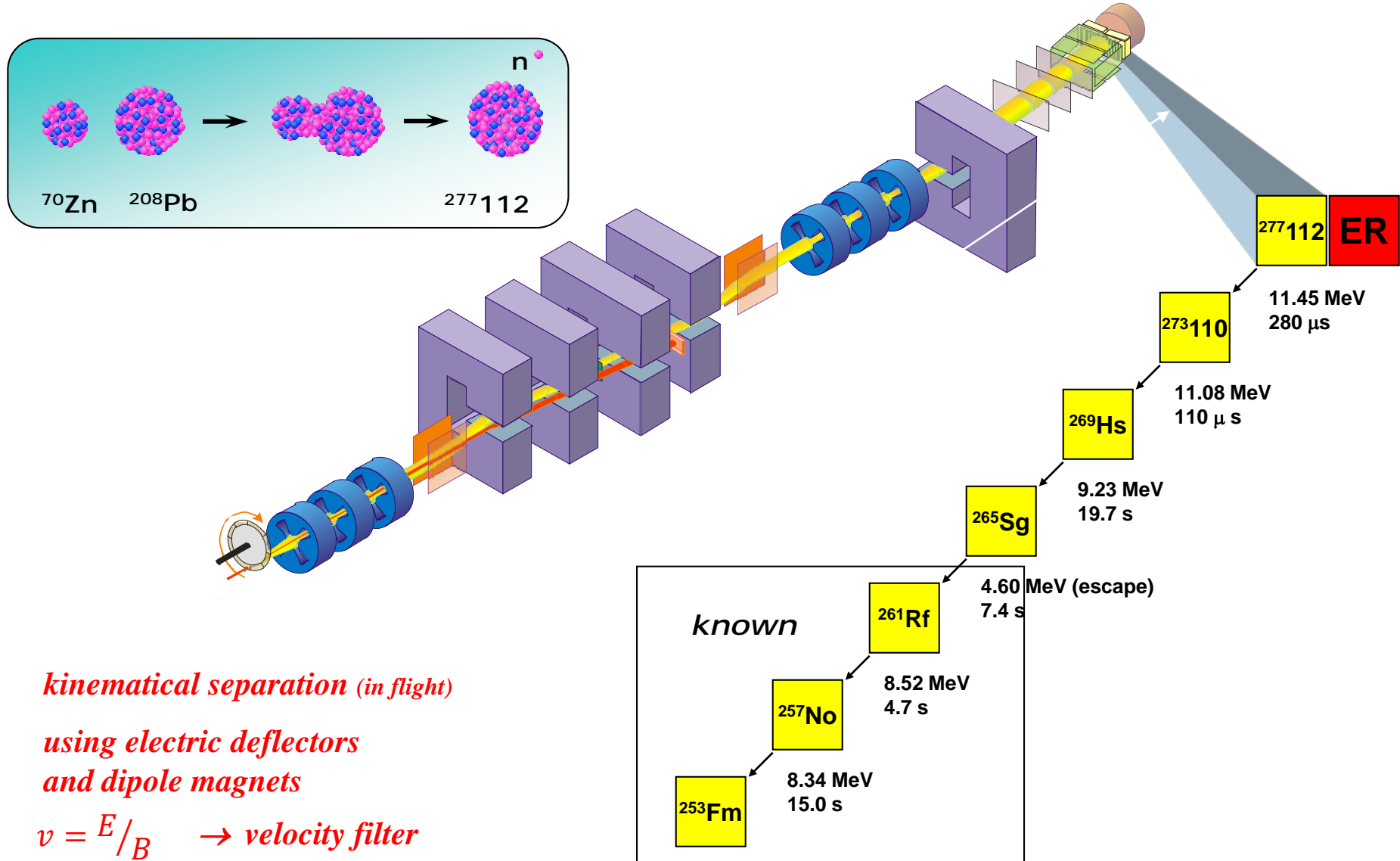
energy resolution $\Delta E = 18-20 \text{ keV}$ @ $E_\alpha > 6 \text{ MeV}$ (cooling 260K)

position resolution $\Delta x = 0.3 \text{ mm}$ (FWHM)

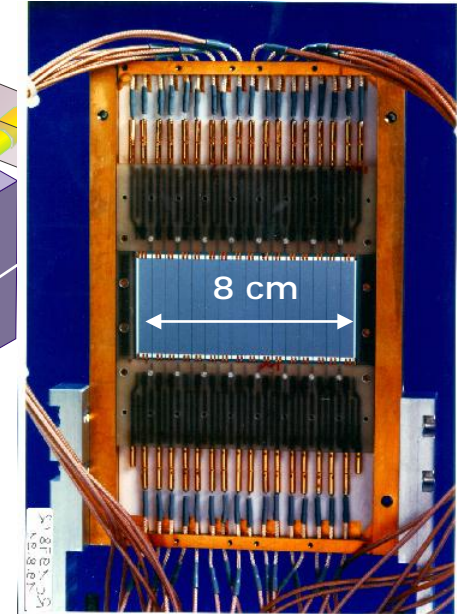
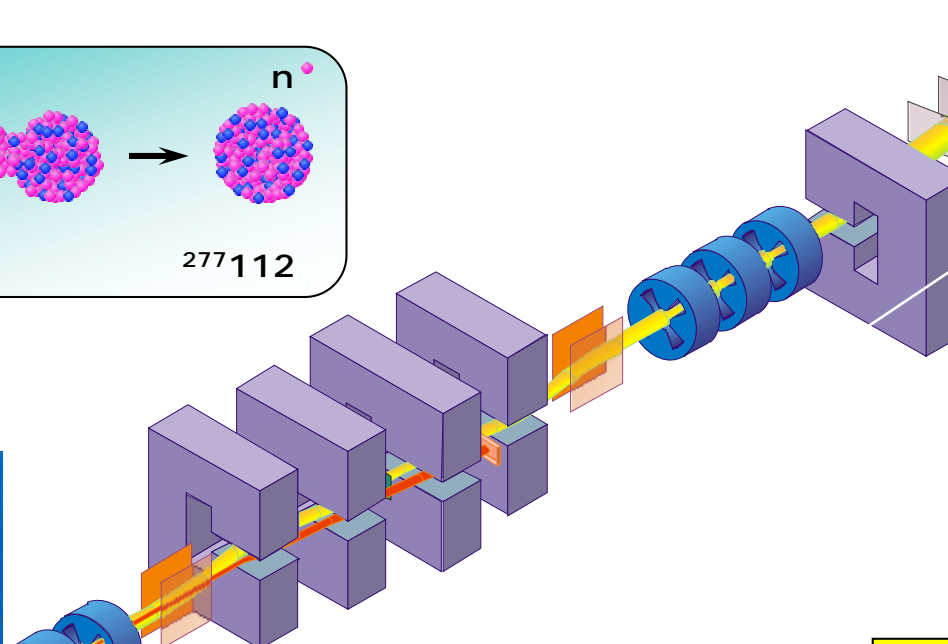
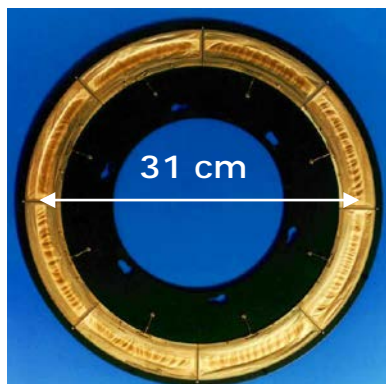
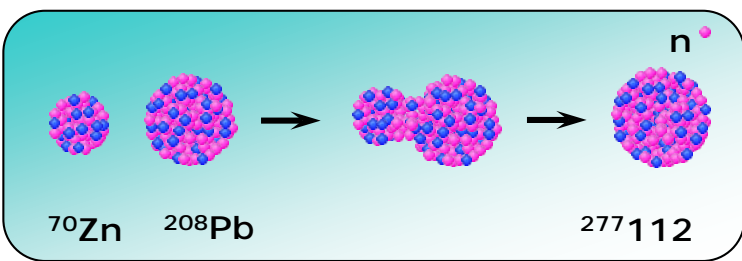
Wait for the emission of an α -particle
(or β -particle)

correlation method: implantation and decay event in the same pixel

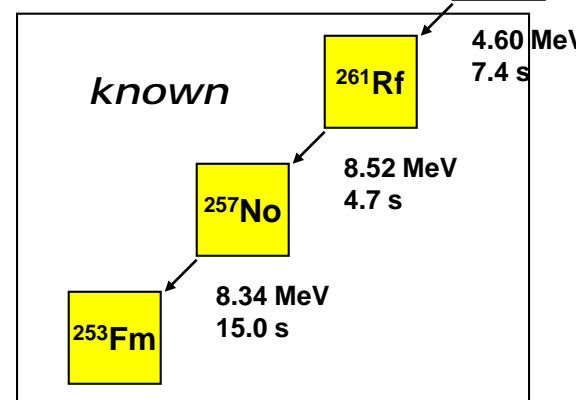
Synthesis and identification of heavy elements with SHIP



Synthesis and identification of heavy elements with SHIP



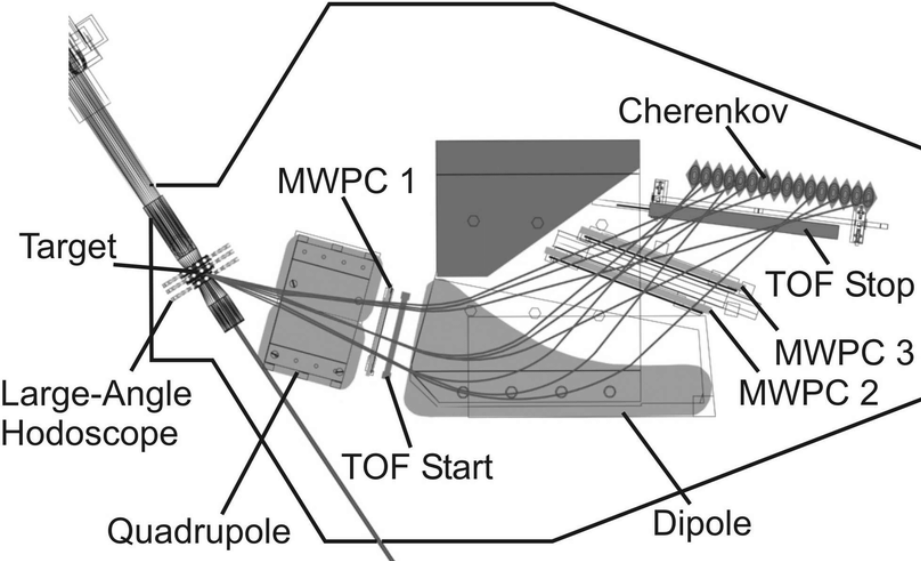
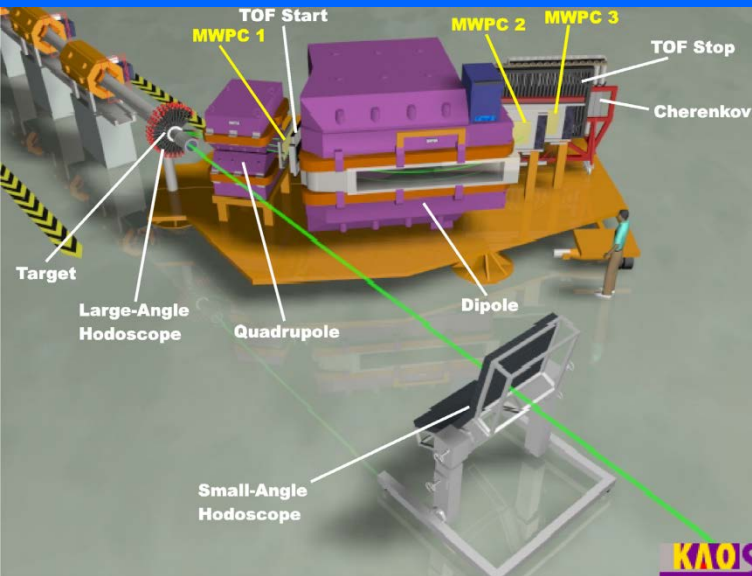
Identification by α - α correlations down to known isotopes



Date: 09-Feb-1996
Time: 22:37 h

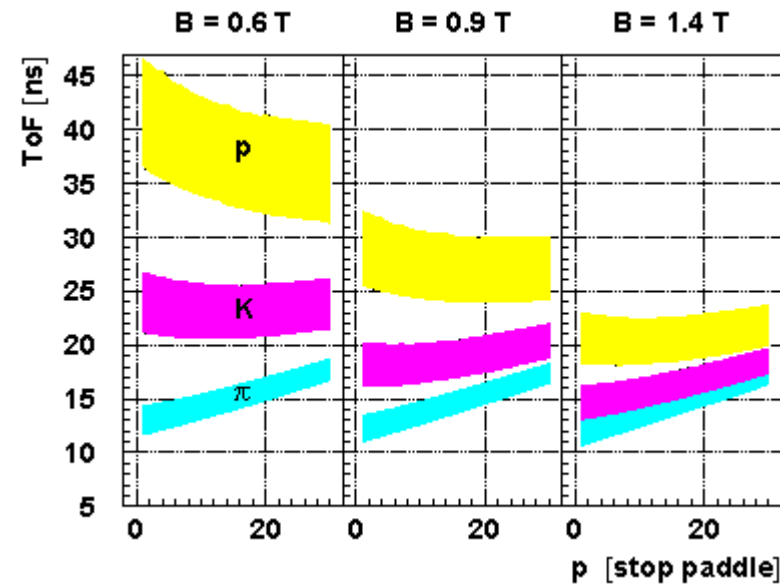
*kinematical separation (in flight)
using electric deflectors
and dipole magnets
 $v = E/B$ \rightarrow velocity filter*

Cherenkov Radiation Threshold Detection - The Kaon Spectrometer

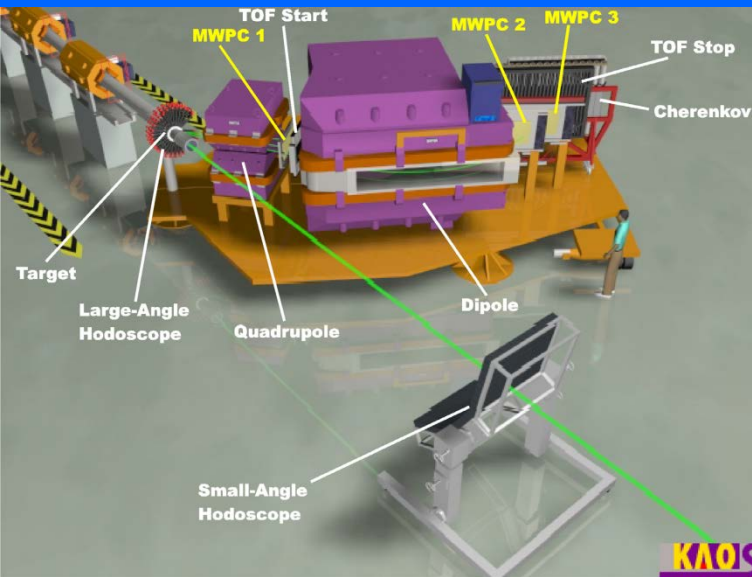


Experimental task is to identify the kaons in a large background of protons and pions.
 p^+, π^+, K^+ rate: $\sim 10000/1000/1$

- ❖ Time-of-flight (ToF) measurement



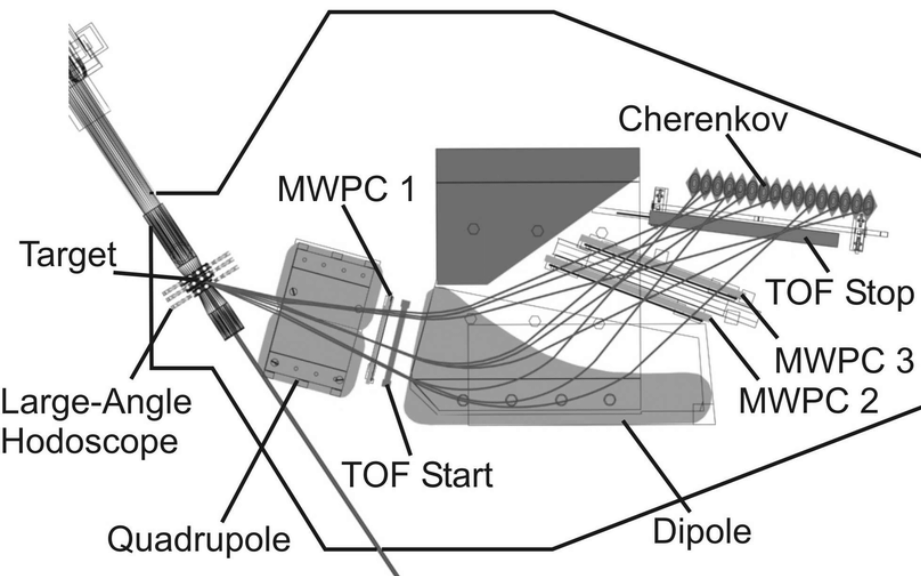
Cherenkov Radiation Threshold Detection - The Kaon Spectrometer



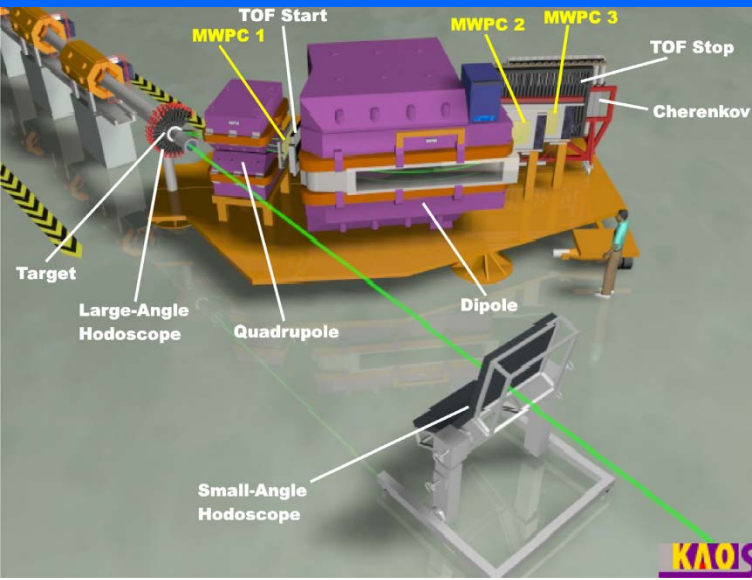
Experimental task is to identify the kaons in a large background of protons and pions.

p^+, π^+, K^+ rate: $\sim 10000/1000/1$

- ❖ Time-of-flight (ToF) measurement
- ❖ Cherenkov detectors
 - 1) lucite ($n = 1.49, \beta \geq 0.67$) and water ($n = 1.34, \beta \geq 0.75$) i.e. above the velocity of protons for $p < 0.8 \text{ GeV}/c$ and $p < 1 \text{ GeV}/c$ respectively
 - 2) silica aerogel ($n = 1.05, \beta \geq 0.95$) allows separation of pions and kaons



Cherenkov Radiation Threshold Detection - The Kaon Spectrometer

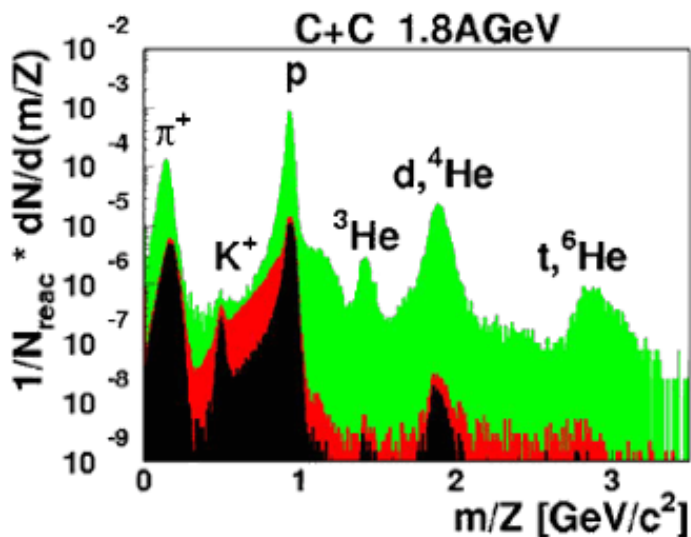


Experimental task is to identify the kaons in a large background of protons and pions.

p^+, π^+, K^+ rate: $\sim 10000/1000/1$

- ❖ Time-of-flight (ToF) measurement
- ❖ Cherenkov detectors
 - 1) lucite ($n = 1.49, \beta \geq 0.67$) and water ($n = 1.34, \beta \geq 0.75$) i.e. above the velocity of protons for $p < 0.8 \text{ GeV}/c$ and $p < 1 \text{ GeV}/c$ respectively
 - 2) silica aerogel ($n = 1.05, \beta \geq 0.95$) allows separation of pions and kaons

The signal from the plastic ToF-wall in coincidence with the first Cherenkov row and in anti-coincidence with the second one can thus be used as a kaon trigger for momenta above $500 \text{ MeV}/c$.



The green spectrum is measured with a trigger on charged particles without ToF.
The red one is measured with the ToF trigger.
The black spectrum is measured with the kaon trigger.